Proceedings of the ASME 2018
Conference on Smart Materials, Adaptive Structures and Intelligent Systems
SMASIS2018
September 10-12, 2018, San Antonio, TX, USA

SMASIS2018-8065

ESTIMATION OF DISTRIBUTION ERRORS IN PIEZOELECTRIC SUBORDINATE OSCILLATOR ARRAYS

Sai Tej Paruchuri[1], **Andrew Kurdila**[2]
Department of Mechanical Engineering
Virginia Tech
Blacksburg, Virginia 24060
Email: [1] saitejp@vt.edu, [2] kurdila@vt.edu

Joseph Vignola[3]
Department of Mechanical Engineering
Catholic University of America
Washington, D.C., 20064
Email: [3] vignola@cua.edu

ABSTRACT

Subordinate Oscillator Arrays (SOAs) have been shown to be effective methods for band-limited vibration attenuation. However, SOAs are very sensitive to error in parameter distributions. Slight disorder in structural parameters can render an SOA ineffective. Recent research has shown that Piezoelectric SOAs (PSOAs) provide an alternative that can limit the degradation of the frequency response function due to the disorder. The capacitive shunts attached to such SOAs can be tuned to change overall electromechanical properties of the SOA post-fabrication. The conventional methods of tuning, which study the Frequency Response Function (FRF) of each oscillator in the array, can be an extremely time-consuming process. To apply a systematic approach to tuning, an estimate of the disorder in structural property distributions can be crucial. In this paper, we discuss a simple and effective methodology to estimate the actual structural parameters and subsequently tune the PSOA to ameliorate the effect of disorder. We derive an adaptive estimation technique for PSOAs and present numerical results that demonstrate improved vibration attenuation of this approach.

INTRODUCTION

Attaching an array of linear oscillators to a mechanical structure can generate a spectrally flat response in the host [1, 2, 3]. These arrays of oscillators are termed Subordinate Oscillator Arrays, or SOAs, in the literature. The isolated natural frequencies of the oscillators in the SOA are concentrated around the natural frequency of the primary structure to achieve a reduced response over a band of frequency. Vignola et al. have shown in [1] that a straightforward approach to design SOAs is to assign a distribution for the nondimensional frequencies of the SOA. The nondimensional frequency of the n^{th} oscillator in the SOA is defined as

$$\beta_n := \sqrt{\frac{\gamma_n}{\alpha_n}}, \tag{1}$$

where γ_n is the ratio of the oscillator and the primary structure stiffness and α_n is the ratio of the oscillator mass to the host structure mass of the n^{th} oscillator in the SOA. In this paper, these constants, β_n, α_n and γ_n are referred to as the nondimensional frequency, mass and stiffness, respectively.

Even though SOAs can be efficient in achieving band-limited vibration attenuation, they are susceptible to disorder in the parameter distributions β, γ, α due to their very low mass ratios [4]. Disorder in the parameter distributions can arise from uncertainty in the structural parameters, manufacturing defects or both. For example, oscillators in the SOAs designed for high frequency and low mass host systems can have thickness of the order of one-hundredth of a millimeter. In such cases, the uncertainty in the structural parameters can be caused due to tolerance limitations of manufacturing techniques like laser cutting, water jet cutting and traditional machining, which can significantly affect the performance of the SOA [4]. Furthermore, the performance of SOAs operating under nonideal conditions like high

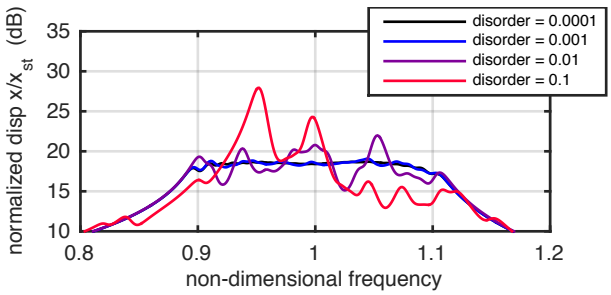

FIGURE 1: Deterioration of the Frequency Response Function with Increasing Disorder in the System, [4]

temperatures can decline over time due to the degradation of its structural properties. Figure 1 shows the effect of increasing error in parameter distributions on the performance of the SOA in [4].

Paruchuri et al. [5,6] proposed tunable Subordinate Oscillator Arrays which have the potential to overcome this limitation. Each oscillator in a tunable SOA is made of a piezoelectric bimorph beam attached to a shunt circuit. The capacitors in the shunt circuit can be tuned to change the open and closed loop stiffness and hence the isolated natural frequency of each oscillator in the array. Even though [5,6] discussed various advantages of such tunable piezoelectric oscillator arrays, they did not explain how piezoelectric oscillators can be tuned to achieve the desired performance in the presence of disorder. The tuning process would require explicit knowledge of the structural properties of the subordinate oscillators, which are unknown. Alternatively, accurate estimates of the structural parameters obtained through parameter estimation techniques can be used to calculate the amount of capacitance that has to be added to or subtracted from the shunt capacitor to achieve attenuation. This approach of tuning can be extended to applications beyond PSOAs. For example, the natural frequency of a piezoelectric energy harvester [7,8] can be tuned to match the excitation frequency to increase the efficiency. In case of artificial hair cell sensors that are capable of mimicking human cochleas behavior [9], each MEMS scale artificial hair can be tuned to have the desired natural frequency in the presence of an error. The next subsection will talk about different parameter estimation techniques considered in the literature.

Structural Parameter Estimation

Traditionally, researchers in the field of control theory developed and implemented a plethora of online parameter estimation techniques for various applications. Vibrations researchers adopted some of these methods for several applications. Some of the earliest works on parameter estimation can be seen in [10,11].

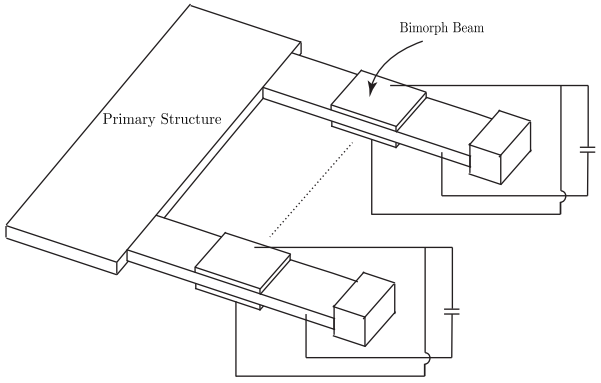

FIGURE 2: A PSOA with capacitive shunt circuit attached to a primary structure.

They adapted a nonlinear filtering algorithm to estimate the mass, stiffness and damping of a portal-frame rig and a squeeze-film isolator. Mohammad et al. in [12] presented a way to estimate the structural parameters of linear as well as nonlinear systems with a single excitation. Bottasso et al. [13] used maximum likelihood estimation based approach to determine the stiffness, mass and inertial properties of a wind turbine blade. TESU et al. in [14] used a poisson moment functional to filter the input data and estimate the structural parameters of a bridge structure. The use of estimation techniques to update the model of a bridge was shown in [15]. Le and Yu [16] presented an approach to estimate the mass and stiffness of a structure using measured acceleration data. Hwang et al. in [17] showed techniques to calculate the natural frequency of a structure by measuring only the output data. The uncertainty involved with the estimation of the frequency response function was modeled in [18,19].

In this paper, we derive an estimator algorithm for the PSOA based on the parallel model adaptive parameter estimation technique [20]. The overall algorithm consists of first estimating the unknown parameters and subsequently redesigning the shunt circuit properties based on these estimates to achieve the desired band-limited response.

PIEZOELECTRIC SUBORDINATE OSCILLATOR ARRAY MODEL

In this section, we present the model of our system that is shown in Figure 2. The equations of motion of a PSOA, consisting of N subordinate oscillators with capacitive shunts, attached to the host structure will have the form

$$\begin{bmatrix} \mathbb{M} & \mathbb{M}_p \\ \mathbb{M}_p^T & \mathbb{M}_{pp} \end{bmatrix} \begin{Bmatrix} \ddot{\mathbb{W}} \\ \ddot{x}_p \end{Bmatrix} + \begin{bmatrix} \mathbb{C} & \mathbf{0} \\ \mathbf{0}^T & C_p \end{bmatrix} \begin{Bmatrix} \dot{\mathbb{W}} \\ \dot{x_p} \end{Bmatrix} + \begin{bmatrix} \mathbb{K} & \mathbf{0} \\ \mathbf{0}^T & k_p \end{bmatrix} \begin{Bmatrix} \mathbb{W} \\ x_p \end{Bmatrix} - \begin{bmatrix} \mathbb{B} \\ \mathbf{0} \end{bmatrix} \mathbb{V} = \begin{bmatrix} \mathbf{0} \\ F_p \end{bmatrix}, \tag{2}$$

$$\mathbb{B}^T\dot{\mathbb{W}} + \mathbb{D}\dot{\mathbb{V}} + \mathscr{C}\dot{\mathbb{V}} = \mathbf{0}. \tag{3}$$

In this equation, x_p is the displacement of the single degree of freedom host structure, $\mathbb{W}$ is the vector of relative displacements of the subordinate piezoelectric oscillators with respect to the host structure, and $\mathbb{V}$ is the vector of voltages across piezoelectric strips in the PSOA. With single mode approximation, $\mathbb{W}$ and $\mathbb{V}$ are $(N \times 1)$ dimensional vectors. The terms $\mathbb{M}$, $\mathbb{C}$, $\mathbb{K}$, $\mathbb{B}$, $\mathbb{D}$ and $\mathscr{C}$ in Equation 2 and 3 are the diagonal matrices of the modal mass, modal damping, modal stiffness, modal control input, piezoelectric capacitance and shunt capacitance of the oscillators in the PSOA, respectively. The term $\mathbb{M}_p$ is the modal mass coupling vector that appears in the model due to the dynamic coupling of the host structure and the PSOA. In Equation 2, the stiffness and the damping of the host structure are represented by k_p and C_p. The term $\mathbb{M}_{pp} := m_p + M_p$, where m_p is the primary mass and M_p is the total modal mass of the PSOA. The term f_p represents the input force applied to the host structure. Detailed derivation of these equations of motion can be found in [5,6]. As expected, Equation 2 looks very similar to the equations of motion of a DVA attached to a single degree of freedom system. As we discuss more fully in the next section, estimation technique will be based on a state space formulation of our governing equations. One such model can be derived directly from Equations 2 and 3 by defining $X = \left\{\mathbb{W}^T, x_p, \dot{\mathbb{W}}^T, \dot{x}_p, V\right\}^T$ and setting

$$\boldsymbol{A} = \begin{bmatrix} \mathbf{0} & \boldsymbol{I} & \mathbf{0} \\ \boldsymbol{M}^{-1}\boldsymbol{K} & \boldsymbol{M}^{-1}\boldsymbol{C} & \boldsymbol{M}^{-1}\boldsymbol{B} \\ \mathbf{0} & (\mathbb{D}+\mathscr{C})^{-1}\boldsymbol{B}^T & \mathbf{0} \end{bmatrix}, \tag{4}$$

$$\boldsymbol{B} = \begin{Bmatrix} \mathbf{0} \\ \boldsymbol{M}^{-1}[0,1]^T \\ \mathbf{0} \end{Bmatrix}. \tag{5}$$

However, it is important to note that the state space formulation defined by Matrices 2 and 3 is not the minimal realization of the system. The integration of Equation 3 with respect to time, under the assumption of zero initial conditions, gives an expression for voltage,

$$\mathbb{V} = -(\mathbb{D}+\mathscr{C})^{-1}\mathbb{B}^T\mathbb{W}. \tag{6}$$

We get a lower order model by substituting the expression for voltage into Equation 2. It has the form

$$\begin{bmatrix} \mathbb{M} & \mathbb{M}_p \\ \mathbb{M}_p^T & \mathbb{M}_{pp} \end{bmatrix} \begin{Bmatrix} \ddot{\mathbb{W}} \\ \ddot{x}_p \end{Bmatrix} + \begin{bmatrix} \mathbb{C} & \mathbf{0} \\ \mathbf{0}^T & C_p \end{bmatrix} \begin{Bmatrix} \dot{\mathbb{W}} \\ \dot{x}_p \end{Bmatrix} + \begin{bmatrix} \bar{\mathbb{K}} & \mathbf{0} \\ \mathbf{0}^T & k_p \end{bmatrix} \begin{Bmatrix} \mathbb{W} \\ x_p \end{Bmatrix} = \begin{bmatrix} \mathbf{0} \\ F_p \end{bmatrix}, \tag{7}$$

where

$$\bar{\mathbb{K}} := \mathbb{K} + \mathbb{B}(\mathbb{D}+\mathscr{C})^{-1}\mathbb{B}^T. \tag{8}$$

The reduced model can also be expressed in term of x_p and V instead of x_p and $\mathbb{W}$. The minimal state space representation of this model can be formulated by defining the states $X = \left\{\mathbb{W}^T, x_p, \dot{\mathbb{W}}^T, \dot{x}_p\right\}^T$ and setting

$$\boldsymbol{A} = \begin{bmatrix} \mathbf{0} & \boldsymbol{I} \\ \boldsymbol{M}^{-1}\bar{\boldsymbol{K}} & \boldsymbol{M}^{-1}\boldsymbol{C} \end{bmatrix}, \qquad \boldsymbol{B} = \begin{Bmatrix} \mathbf{0} \\ \boldsymbol{M}^{-1}[0,1]^T \end{Bmatrix}. \tag{9}$$

This state space representation can be implemented directly in the estimation algorithm. However, we can only estimate $\bar{\mathbb{K}}$ and not $\mathbb{K}$, $\mathbb{B}$ and $\mathbb{D}$. In the latter sections, we present a straightforward approach to estimate $\mathbb{K}$, $\mathbb{B}$ and $\mathbb{D}$. However, this approach can only be used for passive tuning of the system. The approach for active tuning of shunt capacitance would require an RC shunt circuit. The second equation of motion of this system will look like

$$\mathbb{B}^T\dot{\mathbb{W}} + \mathbb{D}\dot{\mathbb{V}} + \mathscr{C}\dot{\mathbb{V}} + \frac{\mathbb{V}}{\mathbb{R}} = \mathbf{0}. \tag{10}$$

The state space representation of the model defined by Equation 2 and 10 lends itself for the estimation of $\mathbb{K}$, $\mathbb{B}$ and $\mathbb{D}$. In the following discussions, we limit ourselves to the passive case.

PARALLEL MODEL ADAPTIVE PARAMETER ESTIMATION

Our online estimation method for PSOAs is based on the parallel model adaptive parameter estimation technique in [20]. We assume that all the states are available for measurement and the input is bounded. In this section, we briefly discuss the proof for PSOA parameter convergence and the corresponding learning laws for parameters. A linear dynamical system can be expressed in the form

$$\dot{\boldsymbol{X}} = \boldsymbol{A}\boldsymbol{X} + \boldsymbol{B}\boldsymbol{U} \tag{11}$$

where $\boldsymbol{X} \in \mathbb{R}^n$ and $\boldsymbol{U} \in \mathbb{R}^m$. To implement the adaptive estimator, we define the parallel estimator model of Equation 11

$$\dot{\hat{\boldsymbol{X}}} := \hat{\boldsymbol{A}}\hat{\boldsymbol{X}} + \hat{\boldsymbol{B}}\boldsymbol{U}. \tag{12}$$

The evolution of the state error $\dot{\boldsymbol{\varepsilon}} := \dot{\boldsymbol{X}} - \dot{\hat{\boldsymbol{X}}}$, obtained by subtracting Equation 12 from Equation 11, has the form

$$\dot{\boldsymbol{\varepsilon}} = \boldsymbol{A}\boldsymbol{\varepsilon} - \tilde{\boldsymbol{A}}\hat{\boldsymbol{X}} - \tilde{\boldsymbol{B}}\boldsymbol{U}, \tag{13}$$

where $\tilde{\boldsymbol{A}} := \hat{\boldsymbol{A}} - \boldsymbol{A}$ and $\tilde{\boldsymbol{B}} := \hat{\boldsymbol{B}} - \boldsymbol{B}$. We define the Lyapunov function

$$V\left(\varepsilon, \tilde{\boldsymbol{A}}, \tilde{\boldsymbol{B}}\right) := \boldsymbol{\varepsilon}^T \boldsymbol{P} \boldsymbol{\varepsilon} + tr\left(\frac{\tilde{\boldsymbol{A}}^T \boldsymbol{P} \tilde{\boldsymbol{A}}}{\gamma_1}\right) + tr\left(\frac{\tilde{\boldsymbol{B}}^T \boldsymbol{P} \tilde{\boldsymbol{B}}}{\gamma_2}\right). \quad (14)$$

The derivative of the Lyapunov function with respect to time has the form

$$\dot{V} = -\boldsymbol{\varepsilon}^T \boldsymbol{Q} \boldsymbol{\varepsilon}, \quad (15)$$

a negative semidefinite function, when we choose the learning laws for the parameters as

$$\dot{\tilde{\boldsymbol{A}}} = \dot{\hat{\boldsymbol{A}}} = \gamma_1 \boldsymbol{\varepsilon} \hat{\boldsymbol{X}}^T, \qquad \dot{\tilde{\boldsymbol{B}}} = \dot{\hat{\boldsymbol{B}}} = \gamma_2 \boldsymbol{\varepsilon} u. \quad (16)$$

This implies that the state errors $\boldsymbol{\varepsilon}$ as well the parameter errors $\tilde{\boldsymbol{A}}$ and $\tilde{\boldsymbol{B}}$ will converge to a constant as time $t \to \infty$, as discussed in detail in [20].

Persistence of Excitation

The learning laws presented in Equation 16 ensure that the parameters converge to a constant. However, to guarantee the convergence to the actual parameters, we have to use an input that is rich enough to excite all the modes of the system. In other words, we require a persistently exciting input. As defined in [20], a piecewise continuous input, $u(t) : R \to R^m$ is persistently exciting in R^m if and only if there exist constants $T > 0$, $c_0 > 0$, and $c_1 > 0$ such that

$$c_1 I_m \geq \frac{1}{T} \int_t^{t+T} \boldsymbol{U}(\tau) \boldsymbol{U}^T(\tau) d\tau \geq c_0 I_m, \forall t \geq 0. \quad (17)$$

In many adaptive estimation applications, it is difficult to guarantee persistence of excitation of the inputs. However, in the case of the adaptive estimation of PSOAs, the experimental excitation can be chosen to satisfy the persistence of excitation condition.

ESTIMATOR IMPLEMENTATION METHODOLOGY

The estimates of the state and input matrices $\boldsymbol{A}$ and $\boldsymbol{B}$ can be obtained using the learning laws presented in the previous section. When the PSOA is attached to a structure with well-defined parameters, the mass, the stiffness and the damping properties of the PSOA can be obtained from the estimates of the matrices $\boldsymbol{A}$ and $\boldsymbol{B}$. However, a straightforward method for the estimation of PSOA's structural properties is achieved by the elimination of the primary structure entirely. The equation of motion, in this case, will simplify to

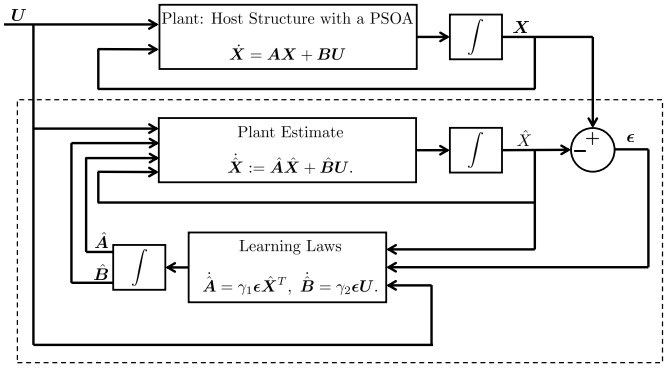

FIGURE 3: Block Diagram of Parallel Model Adaptive Estimator.

$$\mathbb{M}\ddot{\mathbb{W}} + \mathbb{C}\dot{\mathbb{W}} + \bar{\mathbb{K}}\mathbb{W} = \underbrace{-\mathbb{M}_p \ddot{x}_p}_{\mathbb{F}}. \quad (18)$$

The state space formulation of Equation 18 has fewer parameters. Hence, it is easier to choose the adaptive gains γ_1 and γ_2 for the learning laws given in Equation 16 that ensure relatively fast convergence of the parameters. However, it is possible to estimate only the ratios $\mathbb{M}^{-1}\bar{\mathbb{K}}$ and $\mathbb{M}^{-1}\mathbb{C}$ in this case. Capacitance tuning using only the values of $\mathbb{M}^{-1}\bar{\mathbb{K}}$ requires certain approximations which will become apparent in the next section. It is obvious from Equation 8 that the overall stiffness $\bar{\mathbb{K}}$ is a function of the shunt capacitance. If the values of $\bar{\mathbb{K}}$ are known for different values of $\mathscr{C}$, the values of $\mathbb{K}$, $\mathbb{B}$ and $\mathbb{D}$ can be obtained by solving Equation 8. However, as discussed previously, only the values of the ratio $\mathbb{M}^{-1}\bar{\mathbb{K}}$ can be obtained from the estimator. For different shunt capacitances, it is possible to estimate the corresponding values of $\mathbb{M}^{-1}\bar{\mathbb{K}}$. Dividing Equation 8 by the mass estimate of the PSOA $\mathbb{M}$ gives the relation

$$\left\{\hat{\mathbb{M}}^{-1}\hat{\bar{\mathbb{K}}}\right\}_i := \hat{\mathbb{M}}^{-1}\hat{\mathbb{K}} + \hat{\mathbb{M}}^{-1}\hat{\mathbb{B}}(\hat{\mathbb{D}} + \mathscr{C}_i)^{-1}\hat{\mathbb{B}}^T, \quad (19)$$

where $\left\{\hat{\mathbb{M}}^{-1}\hat{\bar{\mathbb{K}}}\right\}_i$ is the ratio corresponding to the capacitance $\mathscr{C}_i$. By running the estimator at least three times for different values of $\mathscr{C}_i$, the above equations can be solved for the values of $(\hat{\mathbb{K}}_n/\hat{\mathbb{M}}_n)$, $(\hat{\mathbb{B}}_n^2/\mathbb{M}_n)$ and $\mathbb{D}_n$ for the n^{th} oscillator in the array. An exact solution can only exist when the parameter errors are precisely zero.

SHUNT CAPACITANCE CALCULATION FOR TUNING

As discussed in the preceding sections, the advantage of using a PSOA is that its effective structural properties can be altered by varying the shunt circuit. Having estimated $(\hat{\mathbb{K}}_n/\hat{\mathbb{M}}_n)$, $(\hat{\mathbb{B}}_n^2/\mathbb{M}_n)$ and $\mathbb{D}_n$ using the techniques presented above, it is now possible to calculate a new shunt capacitance that can give the desired frequency response. In this section, we discuss the calculations involved and the corresponding approximations made for the determination of the new shunt capacitance . The nondimensional frequency distribution of the n^{th} subordinate oscillator in the PSOA, as given in [6], is

$$\beta_n = \sqrt{\frac{\gamma_n}{\tilde{\alpha}_n}}, \tag{20}$$

where $\tilde{\alpha}_n := (\mathbb{M}_n/\mathbb{M}_{pp})$, and $\gamma_n := (\bar{\mathbb{K}}_n/k_p)$. It is important to note the difference in the definition of the nondimensional mass in the SOA and PSOA cases. As shown in [6], one of the PSOA design approaches assigns a discrete distribution for β_n. The presence of uncertainty in structural parameters causes the value of β_n to deviate from the assigned value. We define a new nondimensional frequency distribution in terms of the estimated parameters as

$$\hat{\beta}_n := \sqrt{\frac{\hat{\gamma}_n}{\hat{\tilde{\alpha}}_n}}, \tag{21}$$

where $\hat{\tilde{\alpha}}_n := (\hat{\mathbb{M}}_n/\hat{\mathbb{M}}_{pp})$, $\hat{\gamma}_n := (\hat{\bar{\mathbb{K}}}_n/\hat{k}_p)$, where $\hat{\mathbb{M}}_n$, $\hat{\mathbb{M}}_{pp}$, $\hat{\bar{\mathbb{K}}}_n$ and $\hat{k}_p$ are the estimated values of $\mathbb{M}_n$, $\mathbb{M}_{pp}$, $\bar{\mathbb{K}}_n$ and k_p. Since we cannot estimate the value of the total modal mass of the PSOA, M_p, we cannot calculate $\hat{\beta}_n$. It has been demonstrated in [1] that SOAs can achieve the desired flat frequency spectra at mass ratios as low as 1% or when $m_p \gg M_p$. Hence, we can make the approximation $\mathbb{M}_{pp} \approx m_p$. The new shunt capacitance of the piezoelectric oscillator $\mathscr{C}_{new}$ is chosen such that the value of $\hat{\beta}_n$ matches the value for β_n. We have the relation

$$\hat{\bar{\mathbb{K}}}_n = \hat{\mathbb{K}}_n + \frac{\hat{\mathbb{B}}_n^2}{\hat{\mathbb{D}}_n + \mathscr{C}_{new}}. \tag{22}$$

Equating $\hat{\beta}_n$ with the desired nondimensional frequency β_n result in the expression,

$$\beta_n = \sqrt{\frac{\frac{\hat{\bar{\mathbb{K}}}_n}{\hat{\mathbb{M}}_n}}{\frac{k_p}{m_p}}} = \sqrt{\frac{\frac{\hat{\mathbb{K}}_n}{\hat{\mathbb{M}}_n} + \frac{\hat{\mathbb{B}}_n^2}{\hat{\mathbb{M}}_n(\hat{\mathbb{D}}_n + \mathscr{C}_{new})}}{\omega_p^2}},$$

$$\frac{\hat{\mathbb{B}}_n^2}{\hat{\mathbb{M}}_n(\mathbb{D}_n + \mathscr{C}_{new})} = \beta_n^2\omega_p^2 - \frac{\hat{\mathbb{K}}_n}{\hat{\mathbb{M}}_n},$$

$$\implies \mathscr{C}_{new} = \frac{\frac{\hat{\mathbb{B}}_n^2}{\hat{\mathbb{M}}_n}}{\beta_n^2\omega_p^2 - \frac{\hat{\mathbb{K}}_n}{\hat{\mathbb{M}}_n}} - \mathbb{D}_n. \tag{23}$$

Using Equation 23, we can calculate the new shunt capacitance $\mathscr{C}_{new}$ that will constrain the nondimensional frequency distribution $\hat{\beta}_n$ to the desired value.

Capacitive Tuning Range

One of the important design considerations to consider while designing a piezoelectric oscillator with a shunt capacitor is its capacitive tuning range. Irrespective of the value of the shunt capacitor, the natural frequency of the piezoelectric oscillator with capacitive shunt can take values only within a limited range. The natural frequency of a piezoelectric oscillator with a capacitive shunt is given by

$$\omega = \sqrt{\frac{\mathbb{K} + \frac{\mathbb{B}^2}{\mathbb{D}+\mathscr{C}}}{\mathbb{M}}}. \tag{24}$$

As evident from the above equation, we have the short and open circuit natural frequencies

$$\omega_{n\infty} = \lim_{\mathscr{C}\to\infty} \omega(\mathscr{C}) = \sqrt{\frac{\mathbb{K}}{\mathbb{M}}} \text{ and} \tag{25}$$

$$\omega_{n0} = \lim_{\mathscr{C}\to 0} \omega(\mathscr{C}) = \sqrt{\frac{\mathbb{K} + \frac{\mathbb{B}^2}{\mathbb{D}}}{\mathbb{M}}} \tag{26}$$

respectively. This defines the range of natural frequencies that can be achieved by shunt tuning. The nondimensional frequency of an oscillator in a PSOA $\hat{\beta}_n$ can be tuned to the desired value only when $\hat{\beta}_n \cdot \omega_p$ is within this tunable range.

NUMERICAL RESULTS

The adaptive algorithm was implemented to estimate the structural parameters of a PSOA with one subordinate oscillator. The structural properties of the subordinate piezoelectric oscillator used in simulations were $\mathbb{M}_n = 0.12785$ kg, $\mathbb{C}_n =$

0.0287 Nsec/m, $\mathbb{K}_n = 16.108$ N/m, $\mathbb{B}_n = -6.861e-04$ N/V, and $\mathbb{D}_n = 2.9925e-08$ F, $\beta_n = 1$. Table 1 shows $(\hat{\mathbb{K}}_n/\mathbb{M}_n)$ values obtained after running the adaptive algorithm for 2000 seconds with different shunt capacitances, adaptive gains and inputs. Figures 4, 5 and 6 show the convergence of the entries of the state matrix $\boldsymbol{A}$ and input vector $\boldsymbol{B}$ to the actual values when the plant's shunt capacitance $\mathscr{C}_n = 0$ F. As evident from these figures, the chosen input was sufficient to persistently excite the system and ensure the convergence of the parameter estimates, $\hat{\boldsymbol{A}}$ and $\hat{\boldsymbol{B}}$, to the true values, $\boldsymbol{A}$ and $\boldsymbol{B}$, respectively.

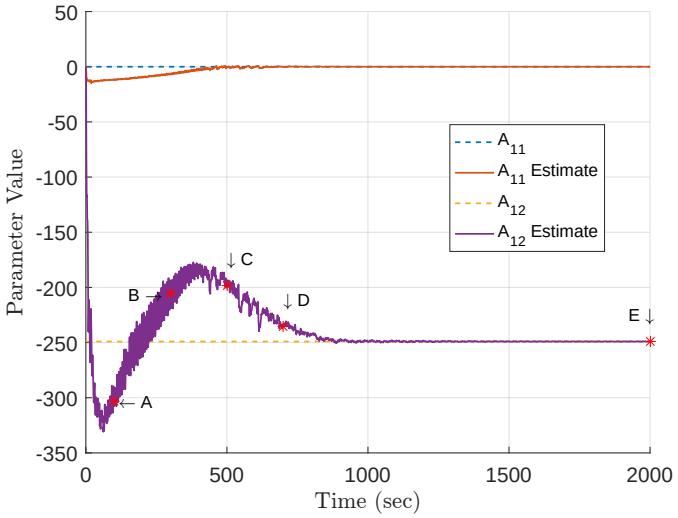

FIGURE 4: The actual values and the corresponding estimates of the elements in the first column of the state matrix $\boldsymbol{A}$ when $\mathscr{C}_n = 0$ F.

Using the different values of $(\hat{\mathbb{K}}_n/\mathbb{M}_n)$ and $\mathscr{C}_n$ given in Table 1, the values of $(\hat{\mathbb{K}}_n/\hat{\mathbb{M}}_n)$, $(\hat{\mathbb{B}}_n^2/\mathbb{M}_n)$ and $\mathbb{D}_n$ were obtained by solving Equation 19. The true and the estimated values of all the parameters are given in Table 2. The new capacitance that matches the natural frequency of the subordinate oscillator with that of the primary structure with mass $m_p = 3.5$ kg, damping $C_p = 0.11047$ Ns/m and stiffness $k_p = 661.25$ N/m was calculated using Equation 23. Table 3 shows the values of $\mathscr{C}_{new}$ calculated using the parameters extracted from the estimator at different times. The frequency response from the force input to the displacement of the actual subordinate piezoelectric oscillator for shunt capacitance values given in Table 3 is shown in Figure 7. Figure 8 shows the frequency response of the primary structure attached to a piezoelectric oscillator with shunt capacitance values given in Table 3. It is evident from the figures that the nondimensional frequency β_n converges to the desired value of 1, as the parameter estimates converge to the actual values.

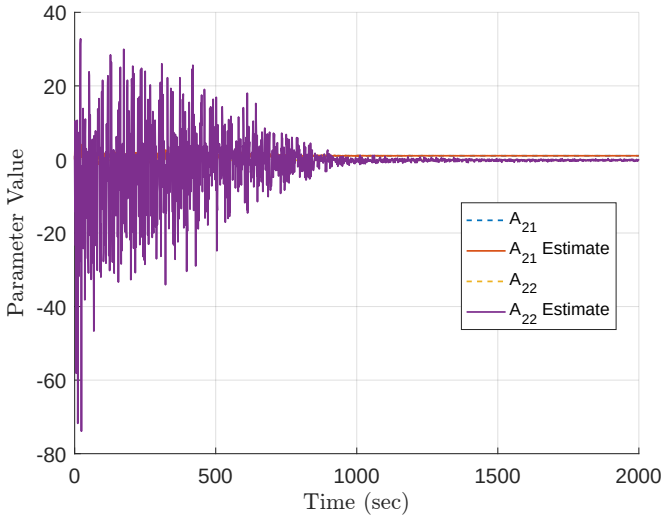

FIGURE 5: The actual values and the corresponding estimates of the elements in the second column of the state matrix $\boldsymbol{A}$ when $\mathscr{C}_n = 0$ F.

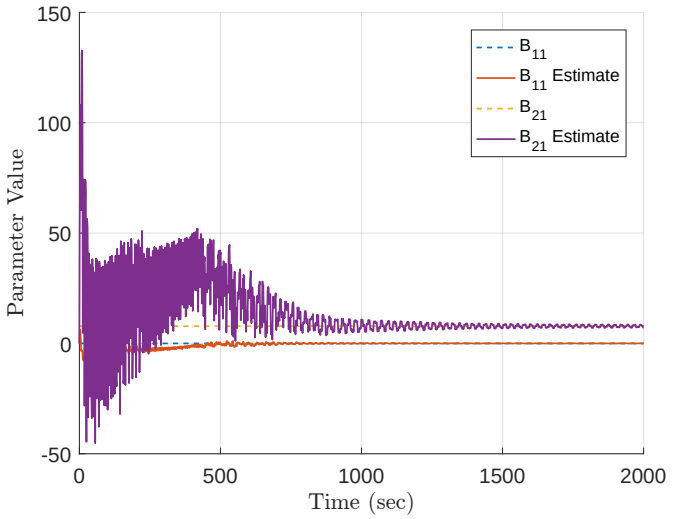

FIGURE 6: The actual and estimated values of the entries in the vector $\boldsymbol{B}$ when $\mathscr{C}_n = 0$ F.

CONCLUSION

This paper presents an approach for determining the shunt capacitance that can produce a PSOA whose frequency response achieves attenuation over a band-limited frequency range. This paper discusses an online algorithm to estimate parameters and modify the structural properties of a piezoelectric subordinate oscillator using a parallel model adaptive estimator. We examine the different approaches for the determination of the structural

$\mathscr{C}_{n,i}$ (Farads)	Input $\boldsymbol{U}$ (N)	Adaptive Gains γ_1, γ_2	$\frac{\hat{\mathbb{K}}_n}{\mathbb{M}_n}\left(\frac{\text{N}}{\text{kg.m}}\right)$
0	$1.5\ (\ \sin 14t + \sin 15t + \sin 16t\ )$	5, 5	248.81
$5e-08$	$1.5\ (\ \sin 13t + \sin 14t + \sin 15t\ )$	6, 6	172.23
1	$1.5\ (\ \sin 10t + \sin 11t + \sin 11t\ )$	3, 3	126.05

TABLE 1: The different values of $(\hat{\mathbb{K}}_n/\hat{\mathbb{M}}_n)$ obtained from the estimator for different shunt capacitance $\mathscr{C}_n$ attached to the piezoelectric oscillator.

Parameters	True	Estimated
$\frac{\mathbb{K}_n}{\mathbb{M}_n}\left(\frac{\text{N}}{\text{kg.m}}\right)$	125.99	126.05
$\frac{\mathbb{B}_n^2}{\mathbb{M}_n}\left(\frac{\text{N}^2}{\text{kg.V}^2}\right)$	$3.682e-06$	$3.701e-06$
$\mathbb{D}_n$ (Farads)	$2.993e-08$	$3.015e-08$

TABLE 2: The true and the estimated values of the structural parameters of the piezoelectric oscillator.

Markers in Figure 4	t (sec)	$\mathscr{C}_{new}$ (*Farads*)
A	100	$4.3389e-08$
B	300	$1.4976e-08$
C	500	$1.6731e-08$
D	700	$2.8445e-08$
E	2000	$2.8716e-08$

TABLE 3: The new shunt capacitance values calculated using Equation 23 after running the estimator for different time periods.

properties of the piezoelectric oscillator from the estimated state-space matrices. Finally, we have presented numerical results for a prototypical example. The results show that the parallel model adaptive estimator is adequate for the determination of structural properties of a piezoelectric oscillator and hence for determining the new shunt capacitance. The adaptive estimator used in this paper requires knowledge of all the states of the system. The techniques discussed in this paper demonstrate the feasibility of

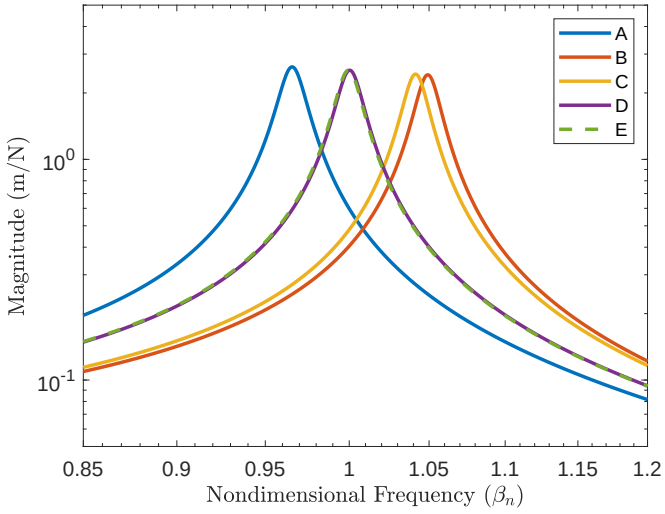

FIGURE 7: The frequency response of the plant attached to different shunt capacitors $\mathscr{C}_{new}$ given in Table 3.

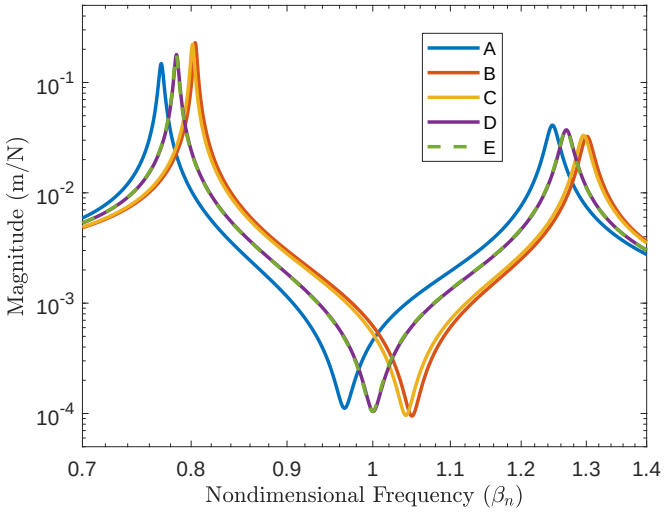

FIGURE 8: The frequency response of the primary structure attached to the subordinate piezoelectric oscillator with shunt capacitances $\mathscr{C}_{new}$ given in Table 3.

implementing estimators for online estimation of structural properties and active tuning of the shunt capacitance.

REFERENCES

[1] Vignola, J. F., Judge, J. A., and Kurdila, A. J., 2009. "Shaping of a system's frequency response using an array of subordinate oscillators". *The Journal of the Acoustical Society of America,* ***126***(1), pp. 129–139.

[2] Zuo, L., and Nayfeh, S. A., 2005. "Optimization of the Individual Stiffness and Damping Parameters in Multiple-Tuned-Mass-Damper Systems". *Journal of Vibration and Acoustics,* ***127***(1), p. 77.

[3] Akay, A., Xu, Z., Carcaterra, A., and Koc, I. M., 2005. "Experiments on Vibration Absorption using Energy Sinks". *The Journal of the Acoustical Society of America,* ***118***(5), p. 3043.

[4] Vignola, J., Judge, J., Sterling, J., Ryan, T., Kurdila, A., Paruchuri, S. T., and Glean, A. "Structural Acoustics and Vibration (others): Paper ICA2016-798 On the use of shunted piezo actuators for mitigation of distribution errors in resonator arrays".

[5] Paruchuri, S. T., Kurdila, A. J., Sterling, J., Vignola, A., Judge, J., Vignola, J., and Ryan, T., 2017. Thermodynamic Variational Formulations of Subordinate Oscillator Arrays (SOA) With Linear Piezoelectrics.

[6] Paruchuri, S. T., Sterling, J., Kurdila, A., and Vignola, J., 2017. "Piezoelectric composite subordinate oscillator arrays and frequency response shaping for passive vibration attenuation". In 2017 IEEE Conference on Control Technology and Applications (CCTA), IEEE, pp. 702–707.

[7] ČEPONIS, A., MAŽEIKA, D., KULVIETIS, G., and YANG, Y., 2018. "Piezoelectric Cantilevers for Energy Harvesting with Irregular Design of the Cross Sections.". *Mechanika,* ***24***(2), mar, pp. 221–231.

[8] Wang, K. F., Wang, B. L., and Zeng, S., 2018. "Analysis of an array of flexoelectric layered nanobeams for vibration energy harvesting". *Composite Structures,* ***187***, pp. 48–57.

[9] Davaria, S., and Tarazaga, P. A., 2017. "MEMS scale artificial hair cell sensors inspired by the cochlear amplifier effect". Vol. 10162, pp. 101620G–10162–10.

[10] Stanway, R., Mottershead, J. E., and Tee, T. K., 1989. "Estimation of mass, damping and stiffness parameters in mechanical vibrating structures". *Transactions of the Institute of Measurement and Control,* ***11***(5), dec, pp. 249–255.

[11] Mottershead, J. E., and Foster, C. D., 1988. "An instrumental variable method for the estimation of mass, stiffness and damping parameters from measured frequency response functions". *Mechanical Systems and Signal Processing,* ***2***(4), pp. 379–390.

[12] Mohammad, K. S., Worden, K., and Tomlinson, G. R., 1992. "Direct parameter estimation for linear and nonlinear structures". *Journal of Sound and Vibration,* ***152***(3), pp. 471–499.

[13] Bottasso, C. L., Cacciola, S., and Croce, A., 2013. "Estimation of blade structural properties from experimental data". pp. 501–518.

[14] TESU, L., ATANASIU, G. M., and COMISU, C.-C., 2016. PARAMETER ESTIMATION IN CONTINUOUS TIME DOMAIN.

[15] Sanayei, M., Khaloo, A., Gul, M., and Necati Catbas, F., 2015. "Automated finite element model updating of a scale bridge model using measured static and modal test data". *Engineering Structures,* ***102***, pp. 66–79.

[16] Le, V., and Yu, T., 2015. "Mass and stiffness estimation using mobile devices for structural health monitoring". Vol. 9437, pp. 94371B–9437–11.

[17] Jae-Seung, H., Dae-Kun, K., and Ahsan, K., 2018. "Estimation of Structural Modal Parameters under Winds Using a Virtual Dynamic Shaker". *Journal of Engineering Mechanics,* ***144***(4), apr, p. 4018007.

[18] Mao, Z., and Todd, M., 2012. "A model for quantifying uncertainty in the estimation of noise-contaminated measurements of transmissibility". *Mechanical Systems and Signal Processing,* ***28***, pp. 470–481.

[19] Mao, Z., and Todd, M., 2013. "Statistical modeling of frequency response function estimation for uncertainty quantification". *Mechanical Systems and Signal Processing,* ***38***(2), pp. 333–345.

[20] Ioannou, P. A., and Sun, J., 1996. *Robust Adaptive Control*. Dover Publications Inc.